The Structure of Methylcob(III)alamin in Aqueous Solution – A Water Molecule as Structuring Element of the Nucleotide Loop

by **Martin Tollinger**, **Robert Konrat**, and **Bernhard Kräutler***

Institute of Organic Chemistry, University of Innsbruck, Innrain 52a, A-6020 Innsbruck, fax: 0043/512/507-2892, e-mail: bernhard.kraeutler@uibk.ac.at

Dedicated to Prof. *Reinhart Keese* on the occasion of his 65th birthday

The solution structure of methylcob(III)alamin (MeCbl; **3**), a natural organometallic corrinoid-B_{12} cofactor whose crystal structure was published in 1985, was established by NMR-spectroscopic analyses of **3** in aqueous solution. The full set of unambiguously assigned ^1H, ^{13}C, and amide ^{15}N signals was consistent with identical constitutional and configurational properties of **3** in solution and in the crystal. Specifically investigated were the conformational characteristics of **3** in solution, in particular of its unique Co-coordinating nucleotide moiety. An extensive set of NOE-derived distance constraints was acquired for this purpose, and of angle constraints, based on three-bond coupling constants. These data were used to calculate the solution structure of **3**. Our data revealed that the conformation of the nucleotide loop of **3** differs significantly in aqueous solution and in the crystalline state and indicated the presence of a specific H_2O molecule 'bound' *via* cooperative H-bonds to three H-bonding functionalities of the nucleotide loop. The observed conformational differences are attributed to structuring contributors to the nucleotide conformation that differ in solution and in the crystal. Most of these can be assigned to H_2O molecules, whose position in the crystal is controlled, in part, by the specific crystal packing.

1. Introduction. – The elucidation of the structure of vitamin B_{12} (=cyanocob(III)-alamin, **1**) [1] by X-ray crystallography and the acquisition of the decisive information on the organometallic nature of coenzyme B_{12} (=(5′-deoxy-5′-adenosyl)cob(III)alamin, **2**) [2] were milestones in structural chemistry (see *Fig. 1*), set by the work from the laboratory of *Hodgkin* [3]. Today still, much of our understanding of the structures and reactivities of vitamin-B_{12} derivatives is based on such single-crystal analyses [4–5] that provide precise structural information (even for reactive, paramagnetic Co^{II} derivatives [6]) in the solid state. In the last dozen years, studies by 2D-NMR spectroscopy of solutions of diamagnetic vitamin-B_{12} derivatives have begun to complement the X-ray crystallographic work [7–9] and have revealed interesting dynamic aspects of the structures of organometallic vitamin-B_{12} derivatives, notably of **2** and of its organometallic moiety [7][9].

A pioneering study in this respect concerned the analysis by combined X-ray and NMR techniques of the structure of methylcob(III)alamin (MeCbl; **3**) [10] (see *Fig. 1*), the simplest organocob(III)alamin. MeCbl (**3**) represents the second type of vitamin-B_{12} coenzymes and organometallic cofactors and is an important reference point for the vitamin-B_{12} field. Methylcorrinoids such as **3** are organometallic methyl-transfer catalysts that are widely distributed in Nature and are employed in important enzymatic methyl-transfer reactions [11]. Therefore, there is strong interest in the structure and in the chemical and spectroscopic properties of **3**. Extensive assignments of signals of the ^1H- and ^{13}C-NMR spectra of **3** were recently published by *Calafat* and *Marzilli* [12], by

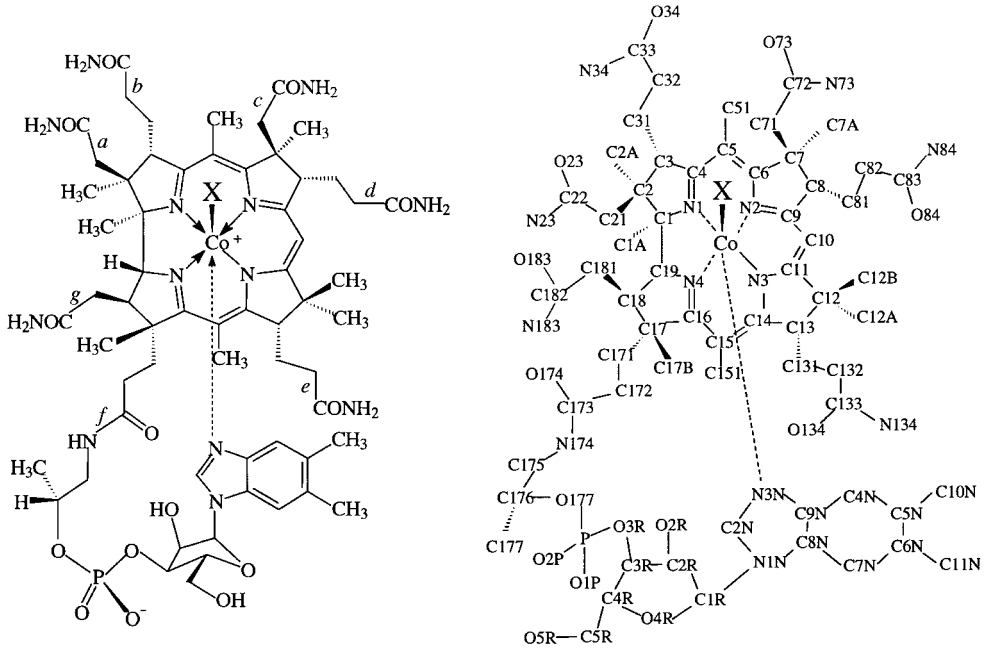

Fig. 1. *Structural formulae of the cob(III)alamins vitamin* B_{12} (**1**, X = CN), *coenzyme* B_{12} (**2**, X = 5′-deoxy-5′-adenosyl), *methylcob(III)alamin* (**3**, X = CH_3), *chlorocob(III)alamin* (**4**, X = Cl), *aquocob(III)alamin cation* ($\mathbf{5}^+$, X = H_2O), *and atom-numbering system used* [5]

Brown et al. [13], and from our laboratory [14]. Based on these, we have now carried out a thorough NMR-spectroscopic analysis of the structure of **3** in aqueous solution at room temperature. A major finding of this study concerns the conformation of the nucleotide loop of **3**: in solution, the nucleotide moiety was found to bind a water molecule *via* multiple and cooperative H-bonding and to adopt a structure significantly different from that in the crystal.

2. Results and Discussion. – 2.1. *Preamble.* The analysis of the structure of methylcob(III)alamin (MeCbl; **3**) in aqueous solution was performed by means of heteronuclear NMR spectroscopy. As a first step towards this goal, a complete assignment of the signals of all (but one of the two exchange-labile OH) protons (65 signals accounting for 90 protons), of all (but two of the corrinato ligand) N-atoms, and of all 63 C-atoms of methylcob(III)alamin (**3**) in its 'base-on' form (at pH 5.5) was achieved recently, by means of complementary sets of two-dimensional gradient-enhanced homo- and heteronuclear experiments [14]. Making use of 'watergate'-ROESY experiments [15][16] that do not require presaturation of the H_2O signal, we were able to detect H_2O-exchangeable protons as well as NOEs to these protons. Accordingly, the assignment of the ^{1}H- and ^{15}N-NMR signals in the spectra of **3** included signals due to all exchangeable amide protons, the corresponding N-atoms, and one OH proton [14]. All spectroscopic data collected for **3** in aqueous solution [10]

[12–14] agreed with and supported the available structural picture of **3** with respect to its constitution and the (relative) configuration of its stereogenic centers.

2.2. *Conformation of the Nucleotide Loop of Methylcob(III)alamin* (**3**). In the crystallographically and spectroscopically characterized (base-on) form of **3**, the nucleotide moiety extends from the *f*-side chain of the corrinato ligand and coordinates intramolecularly to the corrinato-bound Co^{III} centre. It forms the nucleotide loop, unique to 'complete corrins' in their 'base-on' form [1–6]. Particular interest is given to this part of the cobalamin structure, as the Co-coordinating nucleotide moiety is known to modify the reactivity of the metal center in the (organometallic) reactions of **2** and **3** and of other organocobalamins [17–20]. Variability in the nucleotide-loop conformation has mostly been associated with the conformational flexibility of the ribose link, as was established crystallographically by comparison of the available cobalamin crystal structures [3–4] [21]. The discovery of the existence of the base-off forms of **2** and **3** in cobamide-dependent enzymes [11] [22] has spurred further interest in deeper knowledge on the structure and dynamics of the nucleotide segment of the organocobalamins and of other organocobamides [9].

Detailed information concerning the conformational properties in aqueous solution of the nucleotide loop of MeCbl (**3**) was obtained from ROESY data and from three-bond homo- and heteronuclear scalar coupling constants.

ROESY Data: Signals in ROESY experiments represent internuclear cross-relaxation between neighboring protons in the molecule and, therefore, provide information on spatial proximity by comparing distance constraints from the observed NOE intensities with internuclear distances found in the crystal structure of **3**. Due to resonance offset effects in ROESY experiments, NOE enhancements were interpreted in a qualitative manner. Therefore, NOE-derived distance constraints correlate with distance ranges rather than exact distances, *i.e.* strong, medium, and weak NOEs were found for calculated interproton distances in the ranges 2.2–4 Å, 2.5–5 Å, and 3.3–6 Å, respectively.

In detail, NOEs from protons at various sites to H–N(174) and OH–C(2R) provided substantial information about the conformation of the nucleotide loop in solution (for numbering of atoms, see *Fig. 1*). *Fig. 2* shows the cross section through the 200-ms 'watergate' ROESY of **3**, taken at the frequency ω_1 of the *f*-side chain amide proton H–N(174), which exhibits the NOEs with H–N(174). Thus, the NOE between H–N(174) and OH–C(2R) was strong, and that between H–N(174) and H–C(2N) was of intermediate intensity. On the other hand, the NOE between H–N(174) and H_{Si}–C(171) was found to be of little intensity, and that between H–N(174) and H–C(18) could not be detected. In fact, the NOE of H–N(174) to H–C(4R) is five times more intense than the NOE to H_{Si}–C(171) (see *Fig. 2* and *Table 1*). These data are inconsistent with the interproton distances indicated by the crystal structure of **3**: In the crystal H–N(174) points 'outwards', placing H–N(174) at a distance of 4.0 Å from H–C(18), 3.3 Å from H_{Si}–C(171), and 4.0 Å from O(2R). In contrast to the expectations from such distances, the lack of a detectable NOE between H–N(174) and H–C(18), a very weak NOE between H–N(174) and H_{Si}–C(171), as well as a very strong NOE between H–N(174) and OH–C(2R) indicate that the H–N bond is pointing rather 'inwards' into the *f*-loop 'cavity', towards the hydroxy group OH–C(2R). Furthermore, the crystal structure indicates a distance of 4.1 Å between H–N(174) and H–C(4R), in contrast to the NOE of medium intensity between these two protons.

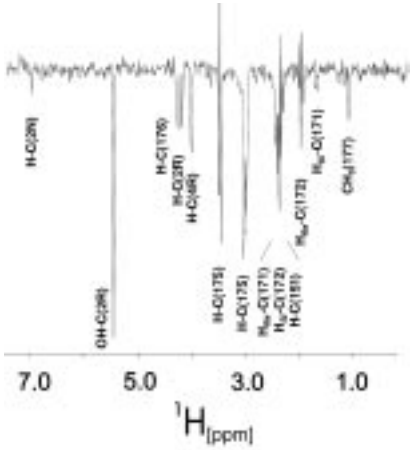

Fig. 2. *Cross section through the 200-ms 'watergate' ROESY of* **3** *at the frequency of the* f*-side chain amide proton H–N(174)*. NOEs are labeled by their proton designations (*Fig. 1*) and are listed in *Table 1*. NOEs at 2.2–2.3 ppm cannot be individually assigned due to overlapping signals of H_{Si}–C(171), H_{Re}–C(172) and H–C(151) and are, therefore, not shown in *Table 1*.

Homo- and Heteronuclear Vicinal Coupling Constants. Vicinal coupling constants were used to determine the magnitude of several decisive dihedral angles, such as ε_i (around the O(3R)–C(3R) bond): P,C-coupling constants between the P-nucleus of the phosphodiester moiety and the atoms C(2R) and C(4R) were obtained from a ^{1}H-decoupled ^{13}C-NMR spectrum. They can be related to the dihedral angle ε_1(P–O(3R)–C(3R)–C(2R)) and ε_2(P–O(3R)–C(3R)–C(4R)) with the RNA *Karplus* relationship for P,C couplings ($^3J(POCC) = 6.9 \cdot \cos^2\varepsilon - 3.4 \cdot \cos\varepsilon + 0.7$) [23]. The P,H-coupling constant between P and H–C(3R) was measured in a ^{31}P-NMR experiment without proton decoupling[1]) and can be related to the angle ε_3(P–O(3R)–C(3R)–H) with the RNA *Karplus* relationship for P,H couplings ($^3J(POCH) = 15.3 \cdot \cos^2\varepsilon - 6.1 \cdot \cos\varepsilon + 1.6$) [24][25]. Experimental coupling constants and calculated values associated to the dihedral angles ε_1, ε_2, and ε_3 are given in *Table 2*. Specifically, the ^3J(C,P) and ^3J(H,P) coupling constants suggest a value of ε_1 close to either $+90$ or $-90°$. However, this ambiguity is resolved, since only one of these dihedral angles ($\varepsilon_1 = +90°$) is compatible with a base-on structure where the dimethylbenzimidazole moiety is attached to the Co-atom [9][10] [12–14]. These data clearly show that ε_1 in the solution structure of **3** amounts to *ca.* 20° less than in the crystal structure of **3**, leading to an 'inwardly' tilted phosphate group.

Qualitative information on the conformation of the α-D-ribose moiety in **3** was derived from vicinal C,H coupling constants ^3J(CH) [24][25], estimated from cross-peak intensities in the PFG-HMBC spectra [14] [26][27]. Six conformationally sensitive dihedral angles H–C–C–C or H–C–O–C are found within the ribose moiety: H–C(1R)–C(2R)–C(3R), H–C(1R)–O(4R)–C(4R), H–C(2R)–C(3R)–C(4R), H–C(3R)–C(2R)–C(1R), H–C(4R)–C(3R)–C(2R), H–

---

[1]) The P,H-coupling constant was deduced from the line splitting in the ^{31}P resonance, which appears as a 1:2:1 *t*.

Table 1. *Diagonal Plot Representing Experimental NOE Intensities Used for the Determination of the Conformation of the Nucleotide Loop in Methylcob(III)alamin* (**3**) (upper part) *and Theoretical* (calculated) *NOE Intensities Deduced from the Solution Structure* (lower part). Experimental NOEs were classified as strong (30–100% rel. intensity), medium (5–30% rel. intensity), and weak 0.5–5% rel. intensity). Strong, medium, and weak NOE correlations are indicated by dark, darkly hatched and lightly hatched fields, respectively. X indicates a scalar coupling (TOCSY artefacts).

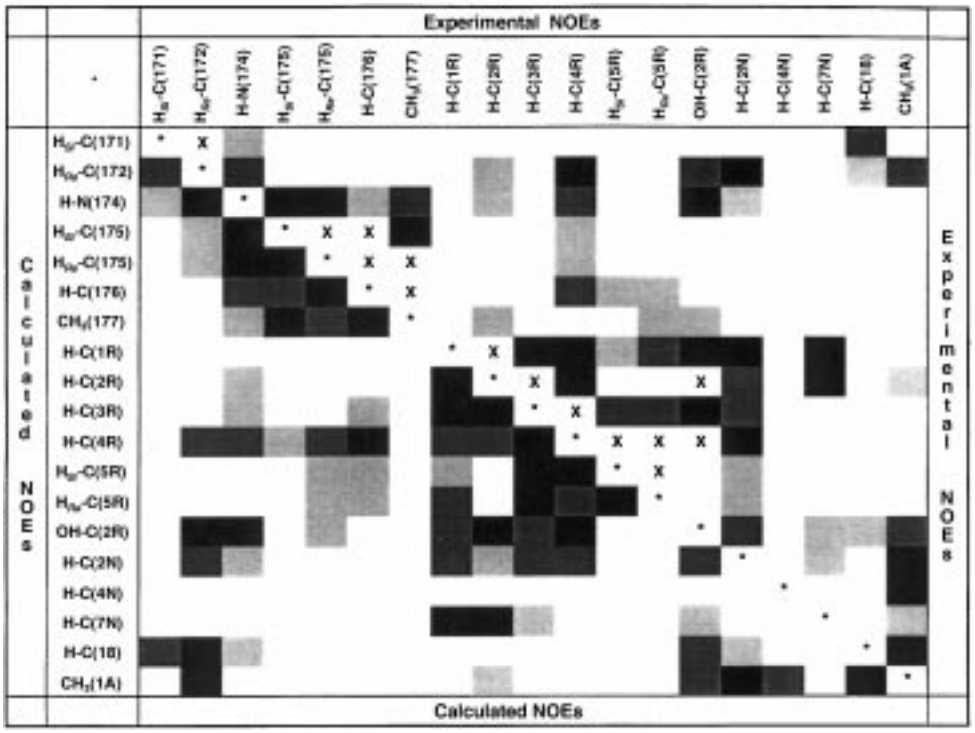

Table 2. *Dihedral Angles* ε_1*(P–O(3R)–C(3R)–C(2R)),* ε_2*(P–O(3R)–C(3R)–C(4R)),* ε_3*(P–O(3R)–C(3R)–H),* θ_1*(H–N(174)–C(175)–*H_{Re}*), and* θ_2*(H–N(174)–C(175)–*H_{Si}*) and Vicinal Coupling Constants* ^{3}J(POCC)*,* ^{3}J(POCH)*, and* ^{3}J(HNCH) *of Methylcob(III)alamin* (**3**). Comparison of results from NMR and X-ray analysis of **3**; coupling constants were calculated with *Karplus* relationships as designed for RNA (^3J(*POCC*), ^3J(*POCH*)) and proteins (^3J(*HNCH*)), respectively.

	Solution structure			**X-Ray structure**	
	^3J (exper.) [Hz]	Dihedral angle [°]	^3J (calc.) [Hz]	Dihedral angle [°]	^3J (calc.) [Hz]
ε_1	< 1	+ 89.1	0.6	+ 112.0	2.9
ε_2	8.5	– 153.0	9.2	– 131.1	5.9
ε_3	7.4	– 34.8	6.9	– 4.5	10.7
Θ_1	5.0	+ 129.2	5.4	– 124.8	4.8
Θ_1	5.0	– 124.2	4.8	– 4.1	7.0

C(4R)–O(4R)–C(1R). None of the corresponding ^3J(C,H) long-range correlation peaks were present in the PFG-HMBC experiment, with the exception of a cross-peak due to $^3J(H–C(2R)–C(3R)–C(4R))$. In the 3′-*endo* conformation, the magnitude of the dihedral angle H–C(2R)–C(3R)–C(4R) is *ca.* 170°, while all other relevant

dihedral angles are close to 90° (between + (75 to 110°) and − (75 to 110°)[2]). Therefore, the ribose unit of **3** in aqueous solution appears to exist in a 3′-*endo* conformation, consistent also with the crystal structure of **3**.

The values of the homonuclear H,H-coupling constants between the amide proton H−N(174) and the two protons H_{Re}−C(175) and H_{Si}−C(175) can be converted into conformational information on the dihedral angles θ_1(H−N(174)−C(175)−H_{Re}) and θ_2(H−N(174)−C(175)−H_{Si}), *i.e.*, into information on θ_i (around the N(174)−C(175) bond at the *f*-side chain), with the protein *Karplus* relationship for N*H*,*H*−C(α) couplings ($^3J(HNCH) = 6.64 \cdot \cos^2\theta - 1.43 \cdot \cos\theta + 1.86$) [28]. The roughly equal coupling of H−N(174) with H_{Re}C(175) and H_{Si}C(175) were deduced from the line splitting of the H−N(174) ^{1}H-resonance which is a 1:2:1 *t*. Although three different conformations around the N(174)−C(175) bond could account for this coupling scheme within the experimental limitations (*ca.* +125°/−125°, *ca.* +35°/+125°, and *ca.* −35°/−125°), NOE-derived distance constraints exclude the latter two possibilities, so that $|\theta_1| \approx |\theta_2| \approx 125°$ (see *Table 2*).

As mentioned above, we detected the ^{1}H-NMR signal of the solvent-exchangeable proton OH−C(2R) of **3** in aqueous solution. This H-atom exchanges remarkably slowly (ca. 4 s^{-1} at pH 5.5) [29], indicating protection from exchange with bulk H_2O. In this situation, favorable to slow exchange, even the determination of a coupling constant between OH−C(2R) and H−C(2R) was possible: the OH resonance was observed as a resolved *d* with a 4.5-Hz splitting at pH 5.5 in 10 mM phosphate-buffer solution[3]). Up to now, only a few $^3J(HOCH)$ coupling constants have been reported [30][31], and a *Karplus* relationship for a similar system is not yet available in the literature[4]). The observed coupling constant of 4.5 Hz for $^3J(HOCH)$ allowed approximate determination of the spatial orientation of OH−C(2R), consistent only with a structure in which OH−C(2R) points roughly towards H−N(174), and suggested a *gauche* conformation (*ca.* 60°) rather than a torsion angle close to 0 or 180° (*Karplus* maxima) or 90° (*Karplus* minimum).

The combination of NOE-derived distance constraints from ROESY experiments and dihedral-angle constraints from coupling constants provided the basis for modeling the (time-averaged) solution structure of the nucleotide loop in methylcob(III)alamin (**3**) as shown (in part) in *Fig. 3*. The structure calculations (Sybyl 6.2, *Tripos Associates*) included all NOE and dihedral-angle constraints (but were independent of H-bonding constraints). In addition, theoretical NOEs were calculated for the solution structure with the full relaxation matrix approach (RMA) [32] as implemented in the computer

---

[2]) Three-bond scalar C,H-coupling constants are expected to follow the general *Karplus* type curve trend, with large values at torsion angles close to 0° or 180° and very small values close to 90°.

[3]) The line splitting was observable only at low phosphate buffer concentrations, *i.e.*, < *ca.* 20 mM. Phosphate catalysis caused broadening of the OH−C(2R) resonance, resulting in a broad signal without detectable line splitting in 100 mM phosphate buffer solutions, which were used for all other NMR experiments. For details, see *Konrat et al.* [29].

[4]) A $^3J(HOCH)$ coupling constant of 10.3 Hz was correlated with a dihedral angle of *ca.* 180° for a threonine residue in the trypsin inhibitor BPTI, while for small coupling constants (< 5 Hz), the dihedral angles have been restricted to ranges excluding the *trans* arrangement of the H−O−C−H moiety by *Wüthrich* and coworkers [30].

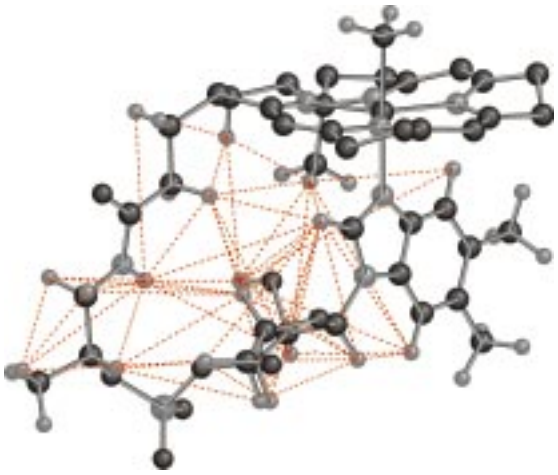

Fig. 3. *Ball-and-stick representation of the nucleotide-loop conformation in the solution, methylcob(III)alamin* (**3**), *including all protons in the nucleotide-loop structure, as well as H–C(19), H–C(20), and the Co-coordinated Me group.* NOEs used for the calculation of this structure are indicated by dotted lines and shown in *Table 1.* Element colours: P large, grey; C medium, black; N medium, grey; O medium, black; Co medium, black; H small, grey.

program Insight II (*Biosym Technologies*). The experimental and calculated NOEs are compared in *Table 1.*

Comparison of the NMR-derived structural data with those from X-ray diffraction studies [10] accordingly reveals major conformational differences in the nucleotide loop between the solution and crystal structures of **3** (see, *e.g.*, *Fig. 4*)[5]). The dihedral angle ε_1 of *ca.* $+90^\circ$ in the solution structure is considerably smaller than that in the crystal structure ($+112^\circ$), while correspondingly ε_2 of *ca.* -150° in the solution structure is considerably more negative than in the crystal structure ($\varepsilon_2 = -131^\circ$). In the solution structure of **3**, the phosphodiester bridge is tilted 'inwards' by *ca.* 20° and towards the 'nucleotide-loop cavity'. The second main difference concerns the conformation of the *f*-side chain. Our observed homonuclear H,H-coupling constants and NOE data suggest an average orientation of the *f*-side chain in which the amide group and H–N(174) point towards the nucleotide-loop 'cavity', with torsional angles τ_1 (C(171)–C(172)–C(173)–N(174)) of 170° and τ_2(C(173)–N(174)–C(175)–C(176)) of 160°. In contrast, in the crystal structure, the amide proton H–N(174) points out of the 'cavity' and towards an H-bonded H_2O molecule there (torsion angles: $\tau_1 = 118.4^\circ$ and $\tau_2 = -97.4^\circ$). As more extensively discussed below, both of these conformational differences between the solution and crystal structure of **3** can be correlated with the formation of H-bonds of the methylcob(III)alamin molecule to H_2O molecules, whose positions differ in the crystal and in aqueous solution.

---

[5]) Aside from conformational differences in the nucleotide loop, on which our discussion focuses, the time-averaged conformations of the flexible amide side chains in solution is not, as a rule, reflected in the corresponding positions in the crystal structures. In particular, the carboxamide function at the *d*-propionamide side chain (C(83), N(84), and O(84)) is shown to be oriented parallel to the plane of the nucleotide base in solution, while it is rotated by about 90° in the crystal, see *Fig. 4* [10].

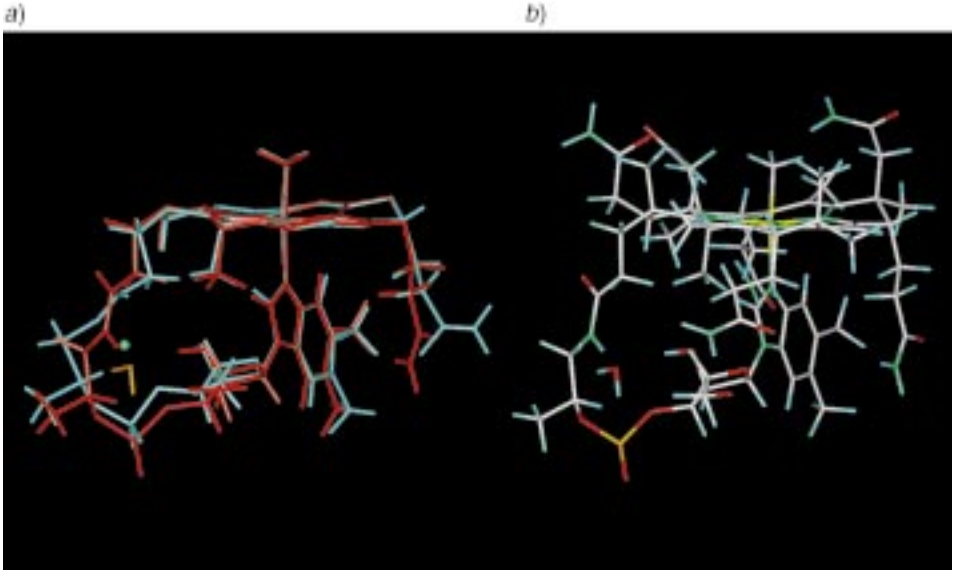

Fig. 4. a) *Overlay of relevant parts of the time averaged structure of* **3** *in aqueous solution* (red), *including the internal bridging H_2O molecule* (orange), *and of the crystal structure of* **3** (light blue) *with the O-atom O(W5)* (green) *of the corresponding H_2O molecule, localized in the crystal structure* (overlay was generated by matching the positions of C(19) and N(4) of the corrinato ligand in the two structures). b) *Model of the time-averaged structure of* **3** *in aqueous solution* (including the bridging H_2O molecule) *as determined by the described NMR-restrained analysis.* Colour coding of atoms: P orange; C white; N green; O red; Co yellow; H light blue.

2.3. *A 'Bound'-Water-Molecule Bridge in the Nucleotide Loop of* **3** *in Aqueous Solution*. The available crystal structures of cobalamins (such as that of MeCbl (**3**) [10], of aquacob(III)alamin [8], and of other 'base-on' vitamin-B_{12} derivatives) reveal the presence of (a) 'conserved' H_2O molecule(s), which is (are) found H-bonded to the phosphate moiety [4]. The published crystal structure of MeCbl (*R* value 15%) [3][10] suffers from considerable disorder of the solvent molecules. A H_2O site has been localized within H-bonding distance to the amide atom N(174). It has been suggested that this H_2O molecule acts as H-bond donor for the ribose hydroxy group OH–C(2R) which, in turn, is a H-bond donor to O(3R), one of the phosphate O-atoms. Both of the terminal phosphate O-atoms O(1P) and O(2P) of **3** are involved in H-bonds only to H_2O molecules that make (external) contacts between symmetry-equivalent molecules of the vitamin-B_{12} derivative [10].

In the following section, we provide experimental evidence for the existence in aqueous solution of an intramolecular H-bonded bridge formed by a single H_2O molecule between the hydroxy group OH–C(2R) of the ribose moiety, the phosphate, and the *f*-amide group of MeCbl (**3**), in contrast to the result derived from the crystal-structure analysis of **3** [10].

H-Bonding of the OH group at the 2-position of the nucleotide ribose unit is clearly manifested by the spectral observation of the proton OH–C(2R) in aqueous solution. The spectral observation of a solvent-exchangeable proton indicates a diminished rate of intermolecular exchange with bulk-H_2O protons due to protection by H-

bonding[6]). The model of relatively strong H-bonding of OH–C(2R) is further supported by the observed difference of the exchange-relayed D/H fractionation factors concerning the two exchange-labile ribose functions OH–C(2R) and OH–C(5R) of MeCbl (**3**) [29]. These findings, first of all, assign to the OH–C(2R) group the role of a H-donor in a strong H-bond. In contrast, the crystallographic results attribute to OH–C(2R) the role of an H-bond acceptor (from the bound H_2O molecule) and of an H-bond donor to the bridging phosphate atom O(3R). The latter H-bond would not be expected to be particularly strong [33].

As mentioned above, the observed value of 4.5 Hz for $^3J(HOCH)$, together with NOE data, restrict the dihedral angle H–O(2R)–C(2R)–H to a nearby *gauche* conformation (*ca.* $+60°$), as shown in *Fig. 4*. In this conformation, no intramolecular H-bond can be formed, since all potential H-bond acceptors (phosphate O-atoms) are not compatible with typical H-bond limitations (lengths of H-bonds and/or bond angles). Therefore, only H-bonding to a H_2O molecule can account for the protection (and the orientation) of the OH group at the 2-position of the ribose moiety in **3**. Assuming an H-bond length of *ca.* 2.8–3.0 Å between the ribose atom O(2R) and the O-atom of H_2O, the H_2O molecule is at a location where it can also form H-bonds to the amide N(174) atom of the *f*-side chain. The position of such a H_2O molecule that is compatible with our experimental data is shown in *Fig. 5*, *a*. The existence of the suggested H-bond to N(174) is supported further by the comparison of ^{15}N-chemical shifts of all amide N-atoms in MeCbl (**3**) in aqueous solution [14] and in dimethyl-sulfoxide solution [34]. A striking feature of these data is that the ^{15}N-resonance of the *f*-amide N(174) occurs at lowest field in aqueous solution, resulting in the chemical-shift sequence *f-a-c-g-e-b-d* of the seven amide N-atoms, while in dimethyl-sulfoxide solution, the resonances of the acetamide N-atoms N(23) and N(73) occur below that of N(174) [9] [34]. ^{15}N-Chemical shifts are very sensitive to H-bonding [35] as well as to solvent effects [36], and the interpretation of ^{15}N-chemical shifts determined in different solvents has to be approached with care. However, the *relative* shift of the ^{15}N-resonance of the *f*-amide is consistent with the formation of a strong H-bond in aqueous solution [37]. The orientation of the amide function (*vide supra*), with the H–N bond pointing 'inwards' into the *f*-loop 'cavity' and towards OH–C(2R), excludes any H-bond acceptor other than the internally bound H_2O molecule, which also acts as H-bond acceptor for the ribose OH group at the 2-position of the ribose moiety.

Taking into consideration optimal H-bond geometries with respect to the distances between H-bonded donor and acceptors (ca. 2.8 Å for O–H···O and ca. 2.7 Å for N–H···O) [33] and the bonding angles at the H-bond H-atom (180°), the two spectroscopically detected H-bonds of the 'internally bound' H_2O molecule (to H–N(174) and H–O(2R)) restrict it to a rather distinct location. In this arrangement, the H_2O molecule would be in good position for the formation of an additional H-bond to the phosphate *pro-R endo* atom O(1P) of the phosphodiester bridge, as shown in *Fig. 5*, *a*. The formation of such an H-bond (between the phosphate *pro-R* O-atom and the 'bound' H_2O molecule) would tend to fix the distance also between the phosphate atom O(1P) and the bridging 'bound' H_2O molecule. The role of the 'bound' H_2O as H-donor in an additional H-bond to the phosphate group in solution requires a distance of

---

[6]) In contrast, the unprotected proton OH–C(5R) is unobservable due to efficient intermolecular exchange.

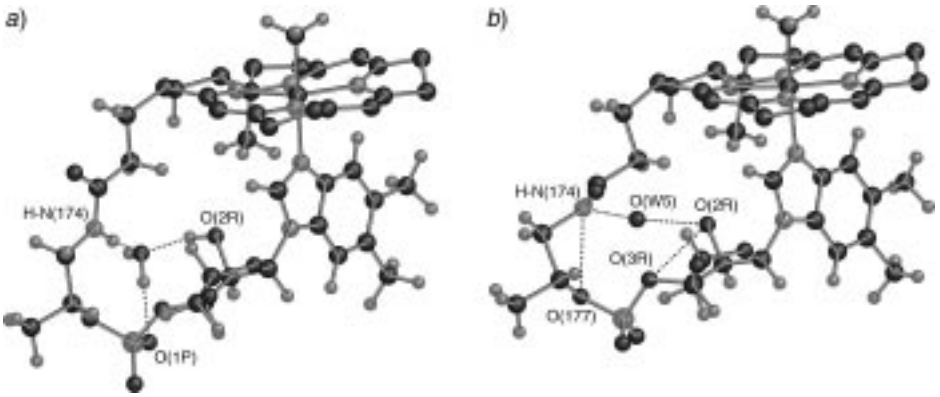

Fig. 5. a) *Internally bound bridging H_2O molecule in the solution structure of* **3***, including the H-bonding network* (H-bonds are indicated by dotted lines; H-bond lengths and H-bond angles: O(2R)–O(water): *ca.* 2.8 Å and *ca.* 160°; N(174)–O(water): *ca.* 2.7 Å and *ca.* 170°; O(P4)–O(water): *ca.* 2.9 Å and *ca.* 180°). b) *Crystal structure of* **3***, including the O-atom of the hydration H_2O molecule W5* (H-bonding contacts and close contacts as suggested by *Rossi et al.* [10] are indicated by dotted lines; H-bond lengths and H-bond angles: O(2R)–O(P3): 2.8 Å; O(2R)–O(W5): 2.9 Å; N(174)–O(W5): 3.1 Å; N(174)–O(177): 2.9 Å)

ca. 3 Å between H_2O and one of the phosphate O-atoms. Such a distance constraint is fulfilled by tilting the phosphate group towards the nucleotide-loop 'cavity', but is incompatible with the conformation of the phosphodiester bridge in the crystal structure of methylcob(III)alamin (**3**) (see *Fig. 5*, *b*). Accordingly, a conformational restructuring of the nucleotide loop in aqueous solution is indicated by the NMR data. This can be rationalized on the basis of a cooperative H-bonding network involving a single 'bound' H_2O molecule. This bridging H_2O molecule serves as proton acceptor for the H-bonds to the ribose proton OH–C(2R), and to the *f*-side chain amide proton H–N(174) and as proton donor in the H-bond to the phosphate *pro*-R *endo* atom O(1P). The combination of the three cooperative H-bonds ($H_2O_{bound}\cdots H-N(174)$, $H_2O_{bound}\cdots HO-C(2R)$ and $O(1P)\cdots H_2O_{bound}$) results in a tetrahedrally coordinated O-center of the involved H_2O molecule and in a strong H-bonding network [33][38].

Most of the crystal structures of 'complete' vitamin-B_{12} derivatives are remarkably conservative with respect to the observed space group ($P2_12_12_1$) and the crystal packing [4][5]. In the crystal, H_2O molecules are typically observed to be involved in H-bonding to the ribose OH–C(2R) and to H-bond ('intramolecularly') either to N(174) (in MeCbl [10]) or to the phosphate *pro-R* atom O(1P) (in the structure of the aquacob(III)alamin cation $\mathbf{5}^+$) [8]. In the crystal structure of $\mathbf{5}^+$, this specific H_2O molecule is also observed to form an 'intermolecular' H-bond to the phosphate *pro-S* atom O(2P) of a symmetry-equivalent B_{12} molecule of $\mathbf{5}^+$ [8]. The crystal structure of MeCbl (**3**) showed both of the terminal phosphate atoms O(1P) and O(2P) to be involved only in such 'intermolecular' H-bonds between symmetry-equivalent molecules of **3** and mediated by H_2O molecules [10]. An alternative scenario involving an H-bonded pair of two bridging H_2O molecules as H-bonding partners of the *f*-amide atom N(174) and the OH–C(2R) has been discovered in the crystal of 10-chloromethylcobalamin [39]. An H-bonded pair of two well characterized H_2O molecules has recently been found also in the crystal structure of chlorocobalamin (**4**)/

lithium chloride [40]: one of these H_2O molecules is H-bonded to N(174) of the *f*-amide and OH–C(2R), while the other contacts the phosphate *pro-R endo* atom O(1P) of the phosphodiester bridge. As observed in both of these crystal structures [39][40], the incorporation of two bridging H_2O molecules allows again for a nucleotide conformation in which the amide moiety directs its H–N(174) out of the nucleotide-loop 'cavity'.

Recently, a different space group ($P2_1$) and a conformation of the nucleotide loop that differs significantly from that in all other crystal structures [1–6][10][39][40] were observed in the crystal of 10-chloroaquacobalamin perchlorate [39]. Remarkably, in this structure, the amide atom N(174) and the ribose OH group are interacting *via* a direct H-bond, and neither of these two centers appears to possess a neighboring, H-bonded H_2O molecule[7]). This finding is an interesting example of a crystal structure of a complete vitamin-B_{12} derivative where both the nucleotide conformation and the crystal packing deviate significantly from what is generally observed in vitamin-B_{12} crystallography.

The observed differences of the nucleotide conformation in the solution and crystal structures of MeCbl (**3**) must be attributed to 'bonding partners' that differ in solution and in the crystal. A factor that is likely to contribute to the generally invariant nucleotide conformation observed in crystals of vitamin-B_{12} derivatives [5] is the existence of H_2O molecules that are H-bonded to the terminal phosphate O-atoms (O(1P), O(2P)) and that mediate 'intermolecular' contacts between symmetry-equivalent molecules [4][5][41]. In this way, the noted preference of the nucleotide conformation of crystalline complete vitamin-B_{12}-derivatives, that crystallize predominantly in the space group $P2_12_12_1$, can be rationalized to arise in part from specific crystal-packing effects. In aqueous solution, H_2O-mediated 'intermolecular' contacts between molecules of vitamin-B_{12} derivatives have not been observed and indeed, they may be considered to be unlikely at the typical concentrations (mM) used for NMR-spectroscopic analysis of these derivatives in aqueous solutions. However, solvation of the ionic phosphate group of cobalamins in aqueous solution (and in crystals of vitamin-B_{12} derivatives grown from aqueous solutions) tends to localize specific ('conserved') H_2O molecules. Even in the known crystal structures of cobamide-dependent enzymes, the phosphodiester moiety of the protein-bound corrinoid cofactors is observed to H-bond to H_2O molecules [11][22].

Conclusions. – An extensive NMR-spectroscopic analysis of the structure of methylcob(III)alamin (MeCbl; **3**) in aqueous solution was used to obtain detailed information on the conformation of the nucleotide moiety of the base-on form of **3** in solution. It revealed conformational properties of the nucleotide loop in aqueous solution that are not consistent with those of the crystal-structure analysis of **3** [10]. The observation of the signals of slowly exchanging amide and OH protons significantly enlarged the experimental basis for the analysis of the solution structure and led to the detection of a 'bound' H_2O molecule linking the polar phosphodiester function, the

---

7) As deduced from the X-ray data, the distance between the amide proton H–N(174) and H–C(4R) of the nucleotide ribose unit amounts to *ca.* 3.5 Å only. Accordingly, the observation of significant NOEs in solution would be expected, in case the nucleotide portion of the solution and crystal structures would closely match each other.

OH–C(R2) group of the ribose moiety, and the amide N-atom of the nucleotide chain of **3** *via* cooperative H-bonds. Such a doubly bridging H_2O molecule, as discovered in the solution structure of MeCbl, appears to be a structural determinant also in coenzyme B_{12} and in other organometallic vitamin-B_{12} derivatives in aqueous solution [9]. While H_2O molecules are typically found in the crystals of 'complete' vitamin-B_{12} derivatives to bind to some of the polar functionalities of the nucleotide portion, they frequently mediate 'intermolecular' contacts between molecules of the vitamin-B_{12} derivative. So far, a H_2O molecule doubly bridging the nucleotide loop *via* three 'internal H-bonds' has not been reported for crystals of vitamin-B_{12} derivatives.

In most of the crystal structures of 'complete' vitamin-B_{12} derivatives (including MeCbl), a strong preference to crystallize in a single space group has been found [4][5]. This correlates with a remarkable conformational invariance of the nucleotide portion and with the existence of an important packing motif. This latter structural motif in the larger part of the crystalline vitamin-B_{12} derivatives involves H-bonded H_2O that mediates intermolecular contacts with the phosphate moiety of the nucleotide moiety.

In the solution and crystal structures of methylcob(III)alamin (**3**), a conformational difference of the nucleotide is observed. Such conformational differences may be systematic for organocobalamins and reflect the existence of the different H-bonding networks in aqueous solution and in the crystal. Crystal packing and the resulting positions of the H-bonded H_2O molecules may thus be assigned a specific restructuring effect in the crystalline solid.

Experimental Part

Materials and Methods. Methylcob(III)alamin **3** was prepared as described in [14]. NMR Experiments: *Varian-500-UNITY-plus* spectrometer with a 5-mm indirect detection probe equipped with field-gradient facilities and a 5-mm broadband direct detection probe; at 26° and 499.887 (^{1}H), 125.15 (^{13}C), or 50.66 MHz (^{15}N); 10 mM solns. of **3** in H_2O/D_2O 9:1, sample size 0.7 ml, pH 5.5, buffered with 100 mM phosphate buffer (unless otherwise stated); signal assignment of ^{1}H-, ^{13}C-, and ^{15}N-resonances by experiments as described in [14]; 1D experiments for the determination of vicinal coupling constants: ^{1}H-NMR using presaturation for solvent suppression, ^{13}C-NMR (^{1}H-broad-band-decoupled) and ^{31}P-NMR; 2D experiments: 'Watergate' *r*otating *f*rame *Overhauser e*nhancement *s*pectroscopy ('watergate'-ROESY) [15][16] and *p*ulsed *f*ield *g*radient *e*nhanced *h*eteronuclear *m*ultiple *b*ond *c*orrelation *s*pectroscopy (PFG-HMBC) [26][27]; all NMR experiments were performed as described in [8] and [14].

Structure Calculations. The solution structure was modelled with the program Sybyl 6.2 (*Tripos Associates*) on the basis of all experimentally observed NOEs and dihedral-angle restraints. The conformation of the nucleotide loop was adjusted manually to satisfy the observed NOE intensities and dihedral-angle restraints. The relative NOE intensities for structurally relevant protons were determined with cross sections through the 200-ms 'watergate' ROESY. This was done separately for each proton of the nucleotide loop. No H-bond restraints were used. As a final step, the structure was minimized using the *Tripos* force-field as implemented in the programme Sybyl 6.2, where the length of the axial Co–N bond was fixed at the crystallographically determined value [10].

The calculation of the theoretical NOEs for the solution structure was performed based on covalently fixed distances and with the full relaxation matrix approach as implemented in the program Insight II (*Biosym Technologies*). An overall correlation time of **3** in aq. soln. of 250 ps [29] was used. The calculated NOEs were classified into three classes corresponding to the relative intensity ranges 30–100% (strong), 5–30% (medium), and $<5\%$ (weak). The experimentally observed NOEs were classified likewise and were compared to calculated ones (see *Table 1*).

We would like to thank Dr. *G. Färber* and Dr. *G. Kontaxis* for help with the computer modelling and NOE simulations. This work was supported by the *Austrian Science Foundation* (Proj. No. 10816 and 11600) and by the *European Union*.

REFERENCES

[1] D. C. Hodgkin, F. R. S. J. Kamper, J. Lindsey, M. MacKay, J. Pickworth, J. H. Robertson, C. B. Shoemaker, J. G. White, R. J. Prosen, K. N. Trueblood, *Proc. Roy. Soc. (London)* **1957**, *A242*, 228.
[2] P. G. Lenhert, D. C. Hodgkin, *Nature (London)* **1961**, *192*, 937.
[3] J. P. Glusker, in 'B_{12}', Ed. D. Dolphin, Wiley, New York, 1982, Vol. 1.
[4] K. Gruber et al.; C. Kratky, in 'Vitamin B_{12} and B_{12} Proteins', Eds. B. Kräutler, D. Arigoni, and B. T. Golding, Wiley-VCH, Weinheim, 1998, p. 335.
[5] C. Kratky, B. Kräutler, in 'Chemistry and Biochemistry of B_{12}', Ed. R. Banerjee, Wiley, New York, in press.
[6] B. Kräutler, W. Keller, C. Kratky, *J. Am. Chem. Soc.* **1989**, *111*, 8936.
[7] A. Bax, L. G. Marzilli, M. F. Summers, *J. Am. Chem. Soc.* **1987**, *109*, 566.
[8] C. Kratky, G. Färber, K. Gruber, K. Wilson, Z. Dauter, H.-F. Nolting, R. Konrat, B. Kräutler, *J. Am. Chem. Soc.* **1995**, *117*, 4654.
[9] R. Konrat, M. Tollinger, B. Kräutler, in 'Vitamin B_{12} and B_{12} Proteins', Eds. B. Kräutler, D. Arigoni, and B. T. Golding, Wiley-VCH, Weinheim, 1998, p. 349.
[10] M. Rossi, J. P. Glusker, L. Randaccio, M. F. Summers, P. J. Toscano, L. G. Marzilli, *J. Am. Chem. Soc.* **1985**, *107*, 1729.
[11] C. L. Drennan, S. Huang, J. T. Drummond, R. G. Matthews, M. L. Ludwig, *Science (Washington, D. C.)*, **1994**, *266*, 1669; C. L. Drennan, M. M. Dixon, D. M. Hover, J. T. Jarrett, C. W. Goulding, R. G. Matthews, M. L. Ludwig, in 'Vitamin B_{12} and B_{12} Proteins', Eds. B. Kräutler, D. Arigoni, and B. T. Golding, Wiley-VCH, Weinheim, 1998, p. 133.
[12] A. M. Calafat, L. G. Marzilli, *J. Am. Chem. Soc.* **1993**, *115*, 9182.
[13] K. L. Brown, D. R. Evans, J. D. Zubkowski, E. J. Valente, *Inorg. Chem.* **1996**, *35*, 415.
[14] M. Tollinger, R. Konrat, B. Kräutler, *J. Mol. Catal. A* **1997**, *116*, 147.
[15] M. Piotto, V. Saudek, V. Sklenár, *J. Biomol. NMR* **1992**, *2*, 661.
[16] A. A. Bothner-By, R. L. Stephens, J.-M. Lee, C. D. Warren, R. W. Jeanloz, *J. Am. Chem. Soc.* **1984**, *106*, 811.
[17] B. Kräutler, *Helv. Chim. Acta* **1987**, *70*, 1268.
[18] B. Kräutler, in 'Vitamin B_{12} and B_{12} Proteins', Eds. B. Kräutler, D. Arigoni, and B. T. Golding, Wiley-VCH, Weinheim, 1998, p. 3.
[19] J. H. Grate, G. N. Schrauzer, *J. Am. Chem. Soc.* **1979**, *101*, 4601.
[20] S. M. Chemaly, J. M. Pratt, *J. Chem. Soc., Dalton Trans.* **1980**, 225.
[21] V. B. Pett, M. N. Liebman, P. Murray-Rust, K. Prasad, J. P. Glusker, *J. Am. Chem. Soc.* **1987**, *109*, 3207.
[22] F. Mancia, N. H. Keep, A. Nakawaga, P. F. Leadlay, S. McSweeney, B. Rasmussen, B. Bösecke, O. Diat, P. R. Evans, *Structure* **1996**, *4*, 339; P. R. Evans, F. Mancia, in 'Vitamin B_{12} and B_{12} Proteins', Eds. B. Kräutler, D. Arigoni, and B. T. Golding, Wiley-VCH, Weinheim, 1998, p. 217.
[23] P. P. Lankhorst, C. A. G. Haasnot, C. Erkelens, C. Altona, *J. Biomol. Struct. Dyns.* **1984**, *1*, 1387.
[24] P. C. Kline, A. S. Serianni, *J. Am. Chem. Soc.* **1990**, *112*, 7373.
[25] C. A. Podlasek, W. A. Stripe, I. Carmichael, M. Shang, B. Basu, A. S. Serianni, *J. Am. Chem. Soc.* **1996**, *118*, 1413.
[26] A. Bax, M. F. Summers, *J. Am. Chem. Soc.* **1986**, *108*, 2093.
[27] R. E. Hurd, B. K. John, *J. Magn. Reson.* **1991**, *91*, 648.
[28] A. C. Wang, A. Bax, *J. Am. Chem. Soc.* **1996**, *118*, 2483.
[29] R. Konrat, M. Tollinger, G. Kontaxis, B. Kräutler, *Monatsh. Chem.*, in print.
[30] E. Liepinsh, G. Otting, K. Wüthrich, *J. Biomol. NMR* **1992**, *2*, 447.
[31] K. Berndt, J. Beunink, W. Schröder, K. Wüthrich, *Biochemistry* **1993**, *32*, 4564.
[32] R. Boelens, T. M. G. Koning, R. Kaptein, *J. Mol. Struct.* **1988**, *173*, 299.
[33] W. Saenger, in 'Principles of Nucleic Acid Structure', Springer Verlag, Berlin, 1984.
[34] K. L. Brown, D. R. Evans, *Inorg. Chem.* **1993**, *32*, 2544.
[35] W. v. Philippsborn, R. Müller, *ibid., Chem.* **1986**, *98*, 381; *ibid. Chem. Int. Ed. Engl.* **1986**, *25*, 383.
[36] G. C. Levy, R. L. Lichter, in 'Nitrogen-15 Nuclear Magnetic Resonance Spectroscopy', Wiley-Interscience, New York, 1979, Chapt. 6.
[37] M. Linas, W. J. Horsley, M. P. Klein, *J. Am. Chem. Soc.* **1976**, *98*, 7554.

[38] J. Bernstein, M. C. Etter, L. Leiserowitz, in 'Structure Correlation', Eds. H.-B. Bürgi, and J. D. Dunitz, Verlag Chemie, Weinheim, 1994, Vol. 2, p. 431 – 507.
[39] K. L. Brown, S. Cheng, X. Zou, J. D. Zubkowski, E. J. Valente, L. Knapton, H. M. Marques, *Inorg. Chem.* **1997**, *36*, 3666.
[40] L. Randaccio, M. Furlan, S. Geremia, M. Slouf, *Inorg. Chem.* **1998**, *37*, 5390.
[41] H. F. J. Savage, P. F. Lindley, J. L. Finney, *Acta Crystallogr., Sect. B* **1987**, *43*, 280.

Received June 10, 1999